Optical Engineering

OpticalEngineering.SPIEDigitalLibrary.org

Pattern effect reduction scheme for high-speed all-optical amplification system

Mohammad Razaghi
Omid Jafari
Narottam K. Das

SPIE.

Pattern effect reduction scheme for high-speed all-optical amplification system

Mohammad Razaghi,[a,*] Omid Jafari,[a] and Narottam K. Das[b,c]
[a]University of Kurdistan, Department of Electrical and Computer Engineering, Sanandaj 66177-15175, Iran
[b]Curtin University, Department of Electrical and Computer Engineering, Miri, Sarawak 98009, Malaysia
[c]Curtin University, Department of Electrical and Computer Engineering, Perth, Western Australia 6845, Australia

Abstract. A method for high-bit-rate optical pulse amplification without a pattern effect (PE) phenomenon is numerically analyzed and presented. In the proposed new scheme, the input signals are applied to a series of 1×2 optical switches and semiconductor optical amplifiers (SOAs). Based on the input signal bit rate and the desired PE reduction rate, it is shown that the number of these devices can be easily optimized. For reducing the SOA nonlinearities on the output signal, a high-birefringent fiber loop mirror is used as an optical Gaussian filter. The achieved results depict that symmetry and the time-bandwidth product of the output signal obtained by this filter are significantly improved. The simulations are performed for high bit-rate signals (>50 Gbps); therefore, in the SOA model, all relevant nonlinear effects that occur in the subpicosecond regimes are taken into account. [DOI: 10.1117/1.OE.53.7.076107]

Keywords: semiconductor optical amplifier; optical demultiplexer; high-birefringent fiber loop mirror; pattern effect; nonlinear effects.

Paper 140493 received Mar. 26, 2014; revised manuscript received Jun. 19, 2014; accepted for publication Jun. 30, 2014; published online Jul. 24, 2014.

1 Introduction

Ultrafast optical systems are required for all-optical signal processing. A semiconductor optical amplifier (SOA) is an important component in these systems mainly due to its specific features, such as high optical gain, small size, and its ability to integrate other semiconductor devices. Therefore, it can be used as pre-, post-, or inline amplifier. In addition, due to nonlinear characteristics of the SOA, it can also be used as a key component in essential optical devices, such as wavelength converters, modulators, and optical logic gates.[1] The main nonlinear effects are self-phase modulation (SPM),[2] interband refractive index dynamics,[3] carrier heating (CH) and spectral hole burning (SHB),[4,5] tow-photon absorption (TPA), ultrafast nonlinear refraction,[6–8] gain dispersion,[9] gain peak shift with the carrier density,[10,11] and the group velocity dispersion (GVD).[12] If repetition rate of input signals is lower than the carrier recovery life time of the mentioned nonlinear effects, the SOA enters to its nonlinear region and cannot properly amplify the input signals as desired for optical communication systems. The carrier recovery life time is ~200 ps.[13,14] The most important drawbacks are the pattern effect (PE) phenomenon and the output pulse's temporal and spectral distortion.[1,15]

Several research works for removing PE have already been performed, such as electronic feedback,[16] using saturable absorber,[17,18] reduction of the carrier life time by injection of continuous wave light,[19,20] clamping of the gain by laser oscillation inside the device,[21,22] using an interferometric method,[23] an optical delay interferometer,[24] using holding light injection,[25] using an asymmetrical Mach–Zehnder interferometer,[26] and using a birefringent fiber loop mirror.[27] However, these methods did not represent a completely satisfactory solution for these issues. The main reason for this is they did not consider all the important nonlinear effects in the SOA.[2–12] Therefore, they cannot predict accurate results for ultrahigh bit-rate input sequences. Besides, based on our proposed new scheme, with some minor changes in the system configuration, theoretically, PE can be entirely removed.

The SOA's nonlinearities also simultaneously distort the time and spectral shape of the picosecond signals.[28] For reducing this distortion, a high-birefringent fiber loop mirror (Hi-Bi FLM) is used as an optical Gaussian filter. With this pulse shaping method, the output signal symmetry is sufficiently improved, while the time-bandwidth product (TBP) of the output signal is considerably increased. This scheme is an inline amplification system, which has been designed to amplify and reshape the high bit-rate data stream without any distortion. The proposed new scheme alternatively divides certain numbers of data bits and amplifies them without the pattern effect. Our proposed new scheme is shown in Fig. 1.

This paper is organized as follows. In Sec. 2, the theoretical analysis and modeling techniques of each part of the proposed configuration (i.e., SOA, Demux, and Hi-Bi FLM) are discussed in detail. The simulation results for a high bit-rate input signal are shown in Sec. 3, and finally, the conclusion is presented in Sec. 4.

2 Theoretical Analysis

2.1 *SOA Model*

In order to include all the important nonlinear effects in the SOA, the following modified nonlinear Schrödinger equation (MNLSE) is used for this modeling:[12,29–31]

*Address all correspondence to: Mohammad Razaghi, E-mail: m.razaghi@uok.ac.ir

0091-3286/2014/$25.00 © 2014 SPIE

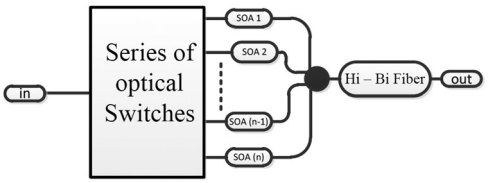

Fig. 1 Schematic of the proposed pattern effect free system.

$$\left[\frac{\partial}{\partial z}-\frac{i}{2}\beta_2\frac{\partial^2}{\partial\tau^2}+\frac{\gamma}{2}+\left(\frac{\gamma_{2p}}{2}+ib_2\right)|V(z,\tau)|^2\right]V(z,\tau)$$
$$=\left\{\left[\frac{1}{2}g_N(\tau)\left[\frac{1}{f(\tau)}+i\alpha_N\right]+\frac{1}{2}\Delta g_T(\tau)(1+i\alpha_T)\right]\right.$$
$$\left.-\left[i\frac{1}{2}\frac{\partial g(\tau,\omega)}{\partial\omega}\bigg|_{\omega_0}\frac{\partial}{\partial\tau}-\frac{1}{4}\frac{\partial^2 g(\tau,\omega)}{\partial\omega^2}\bigg|_{\omega_0}\frac{\partial^2}{\partial\tau^2}\right]\right\}V(z,\tau), \quad (1)$$

where $V(z,\tau)$ is the complex envelope function of an optical pulse. The definitions of parameters in Eq. (1) are as follows:

$$g_N(\tau)=g_0\exp\left[-\frac{1}{E_{\text{sat}}}\int_{-\infty}^{+\infty}u(s)e^{-s/\tau_c}|V(\tau-s)|^2\mathrm{d}s\right], \quad (2)$$

$$f(\tau)=1+\frac{1}{\tau_{\text{shb}}P_{\text{shb}}}\int_{-\infty}^{+\infty}u(s)e^{-s/\tau_c}|V(\tau-s)|^2\mathrm{d}s, \quad (3)$$

$$\Delta g_T(\tau)=\left[-h_1\int_{-\infty}^{+\infty}u(s)e^{-s/\tau_{\text{ch}}}\times(1-e^{-s/\tau_{\text{shb}}})|V(\tau-s)|^2\mathrm{d}s\right.$$
$$\left.-h_2\int_{-\infty}^{+\infty}u(s)e^{-s/\tau_{\text{ch}}}\times(1-e^{-s/\tau_{\text{shb}}})|V(\tau-s)|^4\mathrm{d}s\right], \quad (4)$$

$$\frac{\partial g(\tau,\omega)}{\partial\omega}\bigg|_{\omega_0}=A_1+B_2[g_0-g(\tau,\omega_0)], \quad (5)$$

$$\frac{\partial^2 g(\tau,\omega)}{\partial\omega^2}\bigg|_{\omega_0}=A_2+B_2[g_0-g(\tau,\omega_0)], \quad (6)$$

$$g(\tau,\omega_0)=g_N(\tau,\omega_0)/f(\tau)+\Delta g_T(\tau,\omega_0), \quad (7)$$

where $\tau=t-z/v_g$ is the frame of local time, which propagates with the group velocity (v_g) of the optical pulse at a central angular frequency $\omega_0(=2\pi f_0)$.

The slowly varying envelope function approximation is used in Eq. (1), where the temporal change of the complex envelope function is very slow compared to the cycle of an optical field. Here, the term $|V(z,\tau)|^2$ represents the optical power of an optical pulse, β_2 is the GVD, γ is the linear loss, γ_{2p} is the TPA coefficient, $b_2(=\omega_0 n_2/cA)$ is the instantaneous SPM term due to the Kerr effect, n_2 is an instantaneous nonlinear refractive index, c is the velocity of light in vacuum, $A(=wd/\Gamma)$ is the effective area of the device, d and w are the thickness and width of the active region, respectively, and Γ is the confinement factor.

In addition, $g_N(\tau)$ is the saturated gain due to chromatic dispersion (CD), g_0 is the linear gain, E_{sat} is the saturation energy, τ_c is the carrier lifetime, $f(\tau)$ is the SHB function, P_{shb} is the SHB saturation power, τ_{shb} is the SHB relaxation time, and α_N and α_T are the linewidth enhancement factors associated with the gain changes due to CD and CH, respectively. $\Delta g_T(\tau)$ is the resulting gain change due to CH and TPA, $u(s)$ is the unit step function, τ_{ch} is the CH relaxation time, h_1 is the contribution of stimulated emission and free-carrier absorption to the CH gain reduction, and h_2 is the contribution of TPA. Finally, A_1 and A_2 are the slope and the curvature of the linear gain at ω_0, respectively, while B_1 and B_2 are constants describing the changes in these quantities with saturation.[31]

For solving Eq. (1), the SOA cavity is divided into M equal sections. By using the central-difference approximation in the time domain and trapezoidal integration over the spatial section, and applying an iterative procedure, a set of MNLSEs are solved with high precision in few seconds.[31] The model results are also verified by comparison with the experimental results reported in Refs. 12 and 31.

2.2 *Demultiplexer Model*

For separating the input signal sequence in the time domain regime, a simple demultiplexer (DEMUX) configuration is used as shown in Fig. 2.[32] These DEMUX switching networks consist of a series of 1×2 building blocks, which are generally called a linear bus network. The operation of each of these 1×2 switches is shown in Fig. 3. The suggested 1×2 GaAs/AlGaAs optical switch only uses one multimode interference (MMI) region.[33] This single MMI region works as an MMI coupler by using paired interference

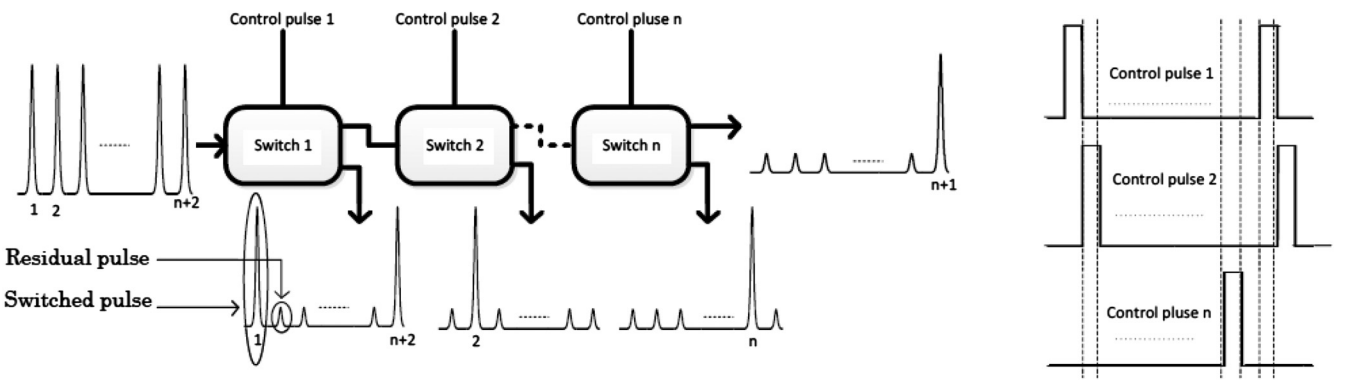

Fig. 2 A simple configuration of optical series switches.

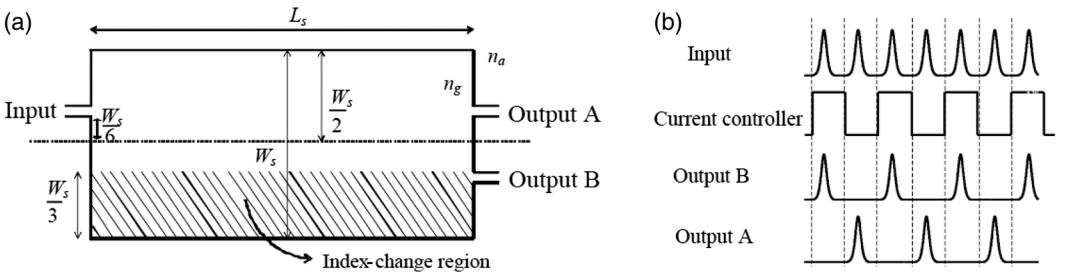

Fig. 3 1 × 2 switch: (a) design[33] and (b) operation.

at the OFF state and symmetric interference at the ON state. By injecting a current of 110 mA, the measured ON/OFF ratio and crosstalk are 23 and 33 dB, respectively, as shown in Fig. 4.[33] Therefore, the residual pulses (as shown in Fig. 2) can be neglected in comparison to the switched pulse. In principle, a carrier injection type switch shall be able to operate at a speed up to gigahertz considering the carrier recombination lifetime in the subnanosecond range; therefore, this switch can satisfy an appropriate operating condition in the proposed new scheme. This switch can also be easily integrated into the AlGaAs/GaAs double heterostructure SOA that is used in our proposed new scheme.

To design suitable switching characteristics for our proposed new PE free system, the length of each switch should satisfy the following equation:[33]

$$L_s \approx \frac{4n_g W_s^2 f_0}{3c}, \tag{8}$$

where n_g is the GaAs refractive index and W_s is the optical switch width.

In this new scheme, based on the desired detached input sequence, the same number of 1 × 2 switches are used as shown in Fig. 2. The amount of the separated input signal should be selected so that the minimum PE occurs after the signal amplification. In this new scheme, using n 1 × 2 switches makes $n+1$ detached pulses. Here, an optimum number of switches is determined by the carrier recovery life time (CRLT) and bit rate (BR). The relationship between the parameters n, CRTL, and BR can be written as $n = \mathrm{CRTL} \times \mathrm{BR}$.

To compensate the insertion loss between switches, the gain of each SOA at the output of the corresponding arm can be adjusted, so that the input energy of all the signals at the input of Hi-Bi FLM becomes identical.

2.3 *Hi-Bi FLM Model*

In order to calculate the transmission field in the Hi-Bi FLM, the well-known method Jones matrix analysis is used.[27] The configuration of a desired Hi-Bi FLM, which acts as an optical filter, is shown in Fig. 5. An equivalent optical circuit of the suggested configuration is also shown in Fig. 6. The Jones matrix analysis for this configuration is defined as follows:

$$[E_{\mathrm{out}}] = \{[K_1][J_{\mathrm{HB}}][K_C] + [K_C][J_{\mathrm{PC}}][K_1]\} \times [J_M] \times \{[K_C][J_{\mathrm{HB}}][K_C] + [K_1][J_{\mathrm{PC}}][K_1]\}, \tag{9}$$

with

$$[J_{\mathrm{PC}}] = \begin{pmatrix} \cos\theta & -\sin\theta \\ \sin\theta & \cos\theta \end{pmatrix} \begin{pmatrix} e^{-i\Gamma_{\mathrm{HF}}/2} & 0 \\ 0 & e^{-i\Gamma_{\mathrm{HF}}/2} \end{pmatrix} \times \begin{pmatrix} \cos\theta & \sin\theta \\ -\sin\theta & \cos\theta \end{pmatrix}$$

$$[J_M] = \begin{pmatrix} 1 & -0 \\ 0 & -1 \end{pmatrix}$$

$$[J_M] = \begin{pmatrix} e^{-i\beta_e L_{\mathrm{HF}}} & 0 \\ 0 & e^{-i\beta_o L_{\mathrm{HF}}} \end{pmatrix},$$

where $[J_{\mathrm{HB}}]$, $[J_M]$, and $[J_{\mathrm{PC}}]$ are the Jones matrix of the Hi-Bi FLM, the mirror, and the polarization controller (PC), respectively. The propagation constant of the e-axis, o-axis, and the length of the Hi-Bi fiber are represented by β_e, β_o,

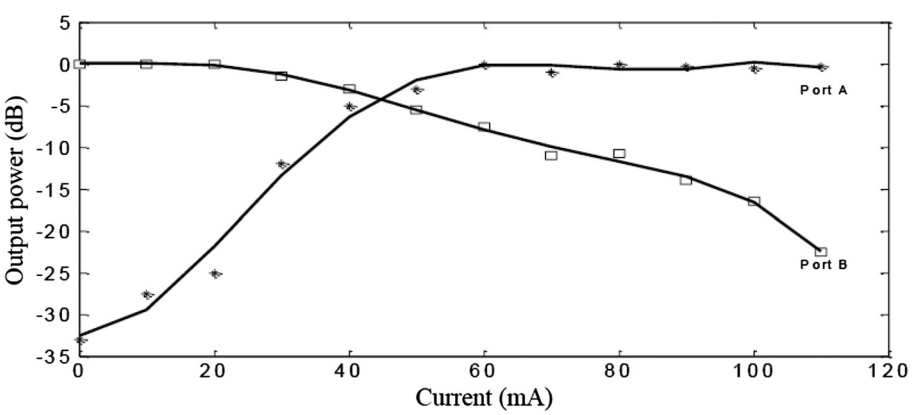

Fig. 4 Switching characteristics of 1 × 2 optical switch.[33]

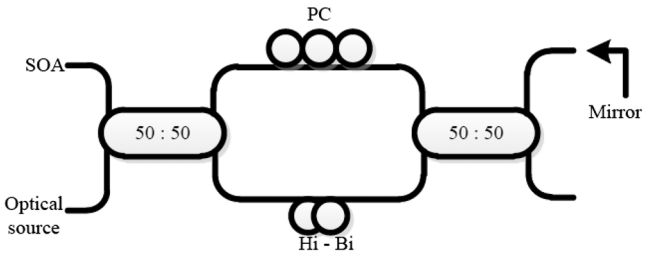

Fig. 5 Schematic setup for the high-birefringent fiber loop mirror (Hi-Bi FLM) configuration.

and L_{HF}, respectively. The difference between the propagation constants β_e and β_o can be represented as

$$\beta_e - \beta_o = \frac{2\pi B}{\lambda}, \tag{10}$$

where $B(= n_e - n_o)$ is the birefringence of the Hi-Bi fiber, Γ_{HF} is the reluctance, and θ represents the orientation of the wave plate axis with respect to the laboratory coordinates. The other matrices are given by

$$[K_1] = [K_{1,3}] = [K_{5,7}] = [K_{4,2}] = \begin{pmatrix} \sqrt{0.5} & 0 \\ 0 & \sqrt{0.5} \end{pmatrix}, \tag{11}$$

$$[K_c] = [K_{1,4}] = [K_{6,7}] = [K_{3,2}] = \begin{pmatrix} i\sqrt{0.5} & 0 \\ 0 & i\sqrt{0.5} \end{pmatrix}, \tag{12}$$

where $[K_1]$ and $[K_c]$ are the coupling and cross-coupling matrices, respectively, for the 3-dB optical coupler.[27] The analytical calculation of the transmitted power spectra of Hi-Bi FLM is shown in Fig. 7, which is in good agreement with the results as reported in Ref. 27.

As the spectral width of SOA's output signal is broader due to the amplification process, by designing the Hi-Bi FLM filter spectral characteristics, the effects of the SOA's nonlinearities can be suppressed.

3 Results and Discussions

Using Fig. 2, the simulation procedure of the proposed scheme can be explained. The first step is the use of the 1×2 switch model at the beginning of each branch. In this way, the model data pulse bit rate is divided by n. Then the output of each switch is considered as the input signal for the SOA model. The SOA modeling technique is based on numerical methods described in Sec. 2.1. The next step is considering the SOA's output pulse as an input for Hi-Bi FLM. Signal propagation in Hi-Bi FLM is then modeled by the Jones matrix analysis approach. As the light propagates in branches of different lengths, synchronization between the demux and re-mux processes can be achieved by using an optical delay line of the desired length in each branch. The parameters used in our simulations are listed in Table 1. The parameters of a double heterostructure AlGaAs/GaAs bulk SOA have been used.[12] The input pulse shapes are sech^2 and they are Fourier transform limited with 0.1 pJ energy. The full width at half maximum of the input pulses is 500 fs with a central frequency of 349 THz.

Figure 8 shows the PE phenomenon after the SOA amplification, where it (in decibel) is defined as the ratio of the maximum peak power (P_{max}) to the minimum peak power (P_{min}) of the amplified output pulse.[28]

$$\text{PE} = 10\log_{10}\left(\frac{P_{max}}{P_{min}}\right). \tag{13}$$

In this case, the 40 bits sample pseudorandom binary using our proposed new scheme is shown in Fig. 9; besides the PE cancellation, SOA's output pulse characteristics, such as spectral width and TBP, are also considerably enhanced.

If the input pulse bit rate is 50 Gbps, the optimum number of switches is equal to $n = 10$ (based on the discussion in Sec. 2.2). Each of these pulses is injected into the SOA connected to the output of each switch. In other words, the input sequence repetition is divided by $n + 1$ at the input of each SOA. Therefore, if $n = 10$, each 1×2 switch and SOA is working at a bit rate of 5 and 4.54 Gbps, respectively. In this bit rate, the SOA gain approximately becomes equal for all the input pulses and the suggested 1×2 switch can operate normally (based on the discussion in Sec. 1). Therefore, PE can be improved considerably and the pulse quality restored for ultrahigh-speed pulses. The results are illustrated in Fig. 9. In this case, the PE is considerably reduced.

As discussed earlier, the residual pulses at the output port of each of the switches are 23 dB weaker than the switched pulses (as shown in Fig. 2). Therefore, using the SOA in the

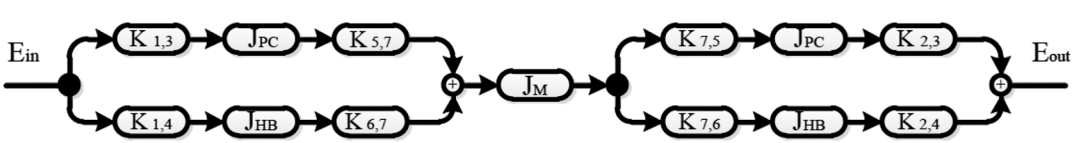

Fig. 6 An equivalent optical circuit of the suggested configuration.

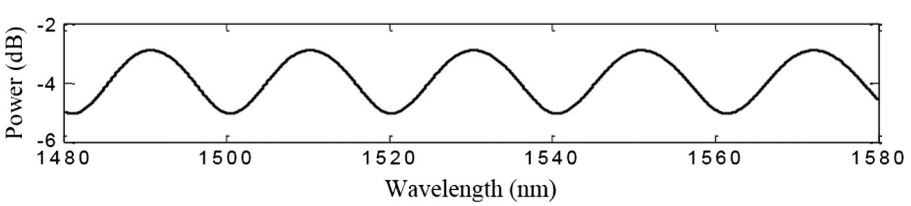

Fig. 7 Spectral response of the Hi-Bi FLM.

Table 1 List of parameters used in simulation.[12,27,33]

Parameters name	Symbol	Value
SOA parameters		
SOA length	L	500 μm
Effective area	A_r	5 μm^2
Center frequency of the pulse	f_0	349 THz
Saturation energy	E_{sat}	80 pJ
Linear gain	g_0	92 cm^{-1}
Group velocity dispersion	β_2	0.05 $ps^2\,cm^{-1}$
Line width enhancement factor due to the carrier depletion	α_N	3.1
Line width enhancement factor due to the carrier heating	α_{ch}	2.0
Contribution of stimulated emission and free-carrier absorption to the carrier heating gain reduction	h_1	0.13 $cm^{-1}\,pJ^{-1}$
Contribution of two-photon absorption	h_2	126 $fscm^{-1}\,pJ^{-2}$
Carrier lifetime	τ_s	200 ps
Carrier heating relaxation time	τ_{ch}	700 fs
Spectral-hole burning relaxation time	τ_{shb}	60 fs
Spectral-hole burning relaxation power	P_{shb}	28.3 W
Linear loss	α_{int}	11.5 cm^{-1}
Instantaneous nonlinear Kerr effect	n_2	$-0.70\ cm^2\,TW^{-1}$
Two-photon absorption coefficient	γ_{2p}	1.1 $cm^{-1}\,W^{-1}$
Parameters describing second-order Taylor expansion of the dynamical gain spectrum	A_2	0.15 $fs\,\mu m^{-1}$
	B_1	−80 fs
	A_1	$-60\ fs^2\,\mu m^{-1}$
	B_2	0 fs^2
Hi-Bi FLM filter parameters		
Orientation of the wave plate axes with respect to the laboratory coordinates	θ	30 deg
Hi- Bi fiber reluctance	Γ_{HF}	76.9
Hi-Bi fiber birefringence	B	8.5e − 5
Propagation constants along the *o*-axis of the Hi-Bi fiber	β_o	1e − 3
Hi-Bi fiber length	L_{HF}	0.36 m
1×2 optical switch parameters		
Width of optical switch	W_s	24 μm
Refractive index of GaAs	n_g	3.24
Refractive index of AlGaAs	n_a	3.22
Length of optical switch	L_s	2900 μm

Note: SOA, semiconductor optical amplifier; Hi-Bi FLM, high-birefringent fiber loop mirror.

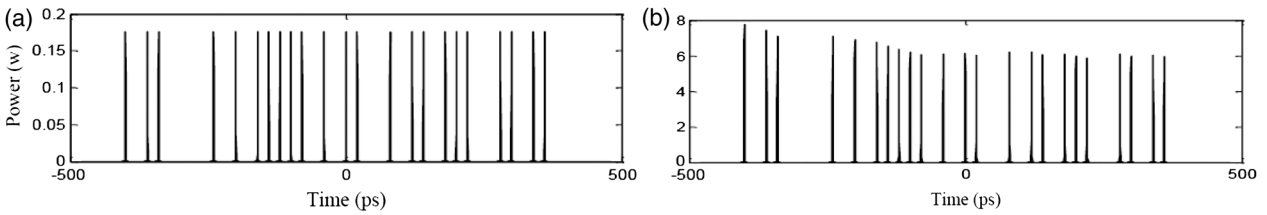

Fig. 8 Temporal waveforms that amplified without applied new scheme: (a) semiconductor optical amplifier (SOA) input and (b) SOA output.

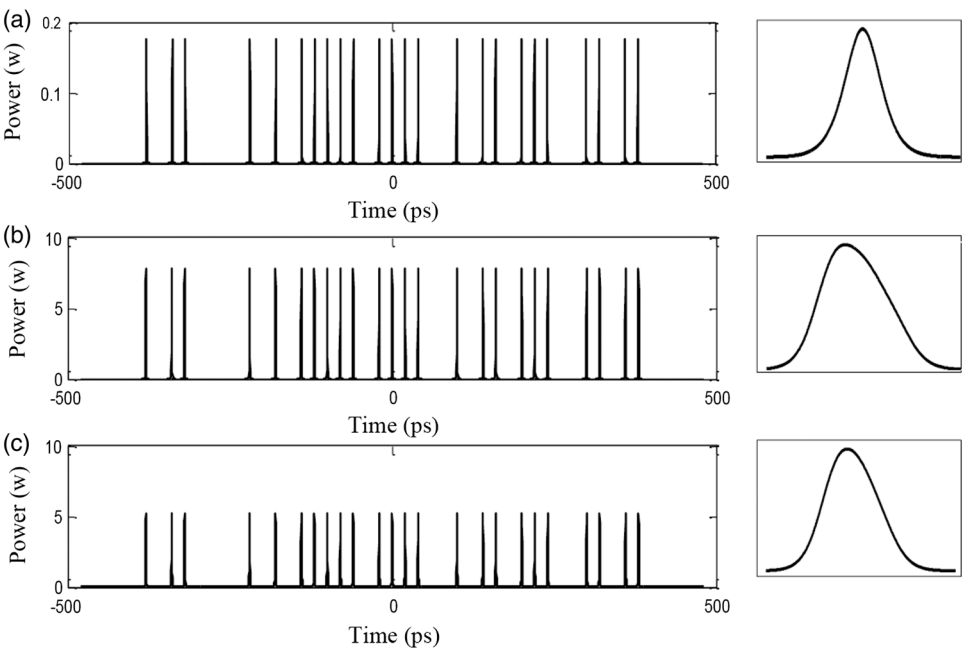

Fig. 9 Temporal waveforms at (a) SOA input, (b) SOA output, and (c) after Hi-Bi FLM. Left column: pseudorandom binary sequence sample of 40 bits. Right column: individual pulse shape.

unsaturated region, the switched pulses are amplified, so their energies are large enough that the amplified residual pulses can be ignored. Thus, the effects of amplified residual pulses in the SOAs' output on the PE can be neglected. The highest bit rate of the proposed system without PE (PE ~ 0) is 50 Gbps if number of switches is equal to 10. It should be noted that by increasing n, the higher input pulse bit rate can also be amplified with a very small PE. If the input pulse's bit rate increases and n remains unchanged, then the PE consequently increases. The detailed result is shown in Fig. 10.

Figure 10 shows the simulation results for $n = 10$ at a bit rate of 100 Gbps input pulse. In this case, the PE for pulses with and without our proposed scheme is 0.271 and 1.849 dB, respectively. By comparing these results, it

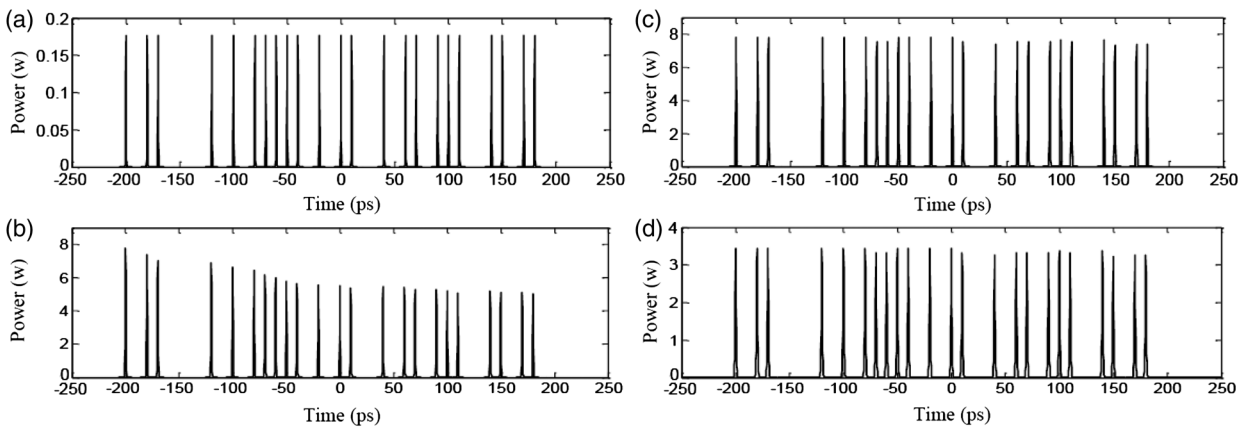

Fig. 10 Temporal waveforms for pulses period of 10 ps at (a) the SOA input, (b) the SOA output without our proposed scheme, (c) the SOA output with our proposed scheme, and (d) output after Hi-Bi FLM.

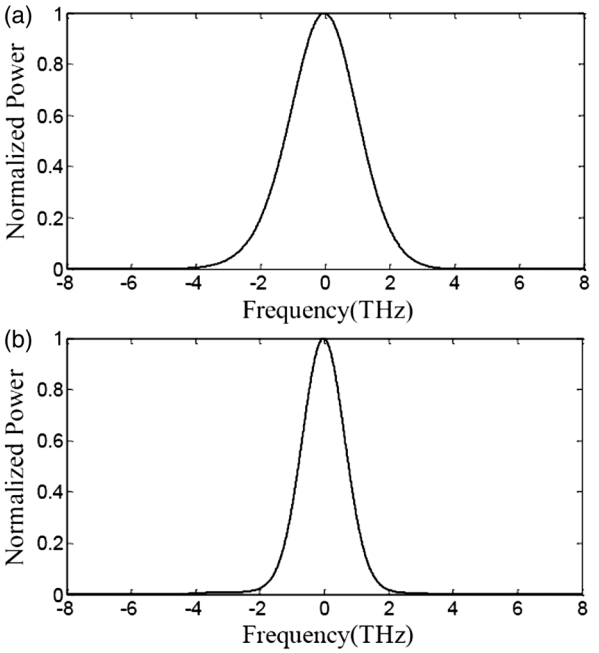

Fig. 11 Optical spectra of output pulse (a) without our proposed scheme and (b) with our proposed scheme.

is concluded that a small amount (<15%) of the PE phenomenon is observed using our proposed new scheme, but it has improved significantly (>85%).

To show the ability of the proposed scheme for PE suppression, an amplified output pulse spectrum of a 50-Gbps data stream is shown in Fig. 11. It is shown that PE and other SOA's nonlinearities, amplification with SOA, broaden the output pulse spectrum [Fig. 11(a)], but by using our proposed scheme, output pulse spectrum is decreased by 63% as shown in Fig. 11(b).

Figure 12 shows the spectra of an input pulse, the SOA's output spectra, and the Hi-Bi FLM output spectra. Due to the gain saturation mechanism of the SOA, its output pulse is asymmetric. This made the output pulse to the leading

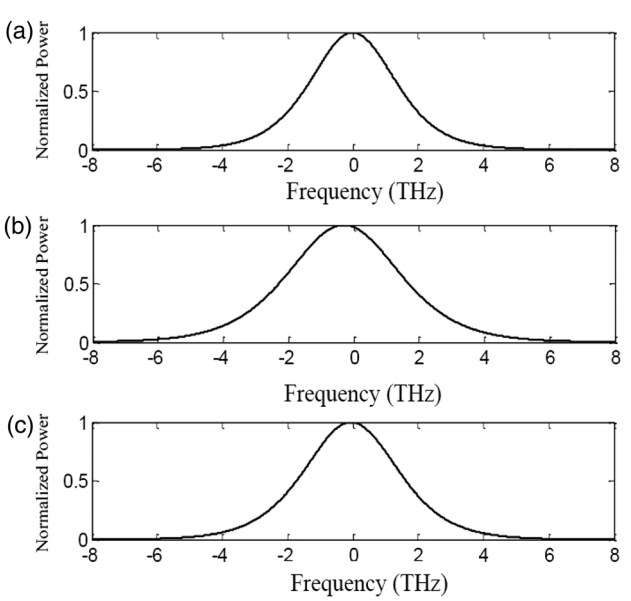

Fig. 12 Optical spectra at (a) SOA input, (b) SOA output, and (c) after Hi-Bi FLM.

edge become sharper than the trailing edge [as shown in Fig. 9(b), right column]. The output pulse spectrum also became broader,[31] as shown in Fig. 12(b). As a result, the output pulse is distorted and its TBP is increased. In order to reduce these effects, the Hi-Bi FLM has been used. This device acts as an optical Gaussian filter. In order to achieve a desirable output, this filter is designed so that it includes 6.6-nm spectral widths at $f_0 = 349$ THz, the central frequency of the input signal. As is shown in Fig. 9(c), right column, this filter makes the output pulse more symmetrical. Furthermore, in this case, the TBP of the output pulse of the Hi-Bi FLM becomes 1.56, which is less than the SOA's output TBP(= 1.956).

4 Conclusion

In summary, a new method for decreasing the PE phenomenon in the amplification process of high-speed optical communication system has been presented. The proposed system consists of a series of optical switches, SOAs, and a Hi-Bi FLM. It has been shown that for 50 Gbps with 10 1×2 switches integrated with SOAs, the PE can be considerably decreased. Besides, using the Hi-Bi FLM as a Gaussian filter improves the SOA's output waveforms, such as its symmetry and TBP. For the model of a high-speed system, all important nonlinear effects relevant to the picosecond and subpicosecond regimes are considered in the SOA. As the SOA and Hi-Bi FLM model results are validated with previously reported results (i.e., published works), the presented numerical model of the proposed system can be reliable and useful for improving the performance of high-speed optical networks.

References

1. M. J. Connelly, *Semiconductor Optical Amplifiers*, Kluwer, Boston, MA (2002).
2. G. P. Agrawal and N. A. Olsson, "Self-phase modulation and spectral broadening of optical pulses in semiconductor laser amplifier," *IEEE J. Quantum Electron.* **25**(11), 2297–2306 (1989).
3. L. Schares et al., "Phase dynamics semiconductor optical amplifiers at 10–40 GHz," *IEEE J. Quantum Electron.* **39**(11), 1394–1408 (2003).
4. A. Mecozzi and J. Mørk, "Saturation effect in nondegenerate four-wave mixing between short optical pulses in semiconductor laser amplifier," *IEEE J. Sel. Topics Quantum Electron.* **3**(5), 1190–1207 (1997).
5. P. Borri et al., "Measurement and calculation of the critical pulsewidth for gain saturation in semiconductor optical amplifier," *Opt. Commun.* **164**(1–3), 51–55 (1999).
6. R. S. Grant and W. Sibbet, "Observation of ultrafast nonlinear refraction in an InGaAsP optical amplifier," *Appl. Phys. Lett.* **58**(11), 1119–1121 (1991).
7. M. Y. Hong et al., "Subpicosecond pulse amplification in semiconductor laser amplifier: theory and Experiment," *IEEE J. Quantum Electron.* **30**(4), 1122–1131 (1994).
8. J. M. Tang and K. A. Shore, "Strong picosecond optical amplifier at transparency," *IEEE J. Quantum Electron.* **34**(7), 1263–1269 (1998).
9. K. Obermann et al., "Performance analysis of wavelength converters based on cross-gain modulation in semiconductor optical amplifier," *J. Lightwave Technol.* **16**(1), 78–85 (1998).
10. Y. Kim et al., "Analysis of frequency chirping and extinction ratio of optical phase conjugate signals by four-wave mixing in SOA's," *IEEE J. Sel. Topics Quantum Electron.* **5**(3), 873–879 (1999).
11. A. E. Willner and W. Shieh, "Optical spectral and power parameters for all-optical wavelength shifting: signal stage, fanout, and cascadability," *J. Lightwave Technol.* **13**(5), 771–778 (2000).
12. N. K. Das, Y. Yamayoshi, and H. Kawaguchi, "Analysis of basic four-wave mixing characteristics in semiconductor optical amplifier by the finite-difference beam," *IEEE J. Quantum Electron.* **36**(10), 1184–1192 (2000).
13. M. Y. Hong et al., "Subpicosecond pulse amplification in semiconductor laser amplifier: theory and experiment," *IEEE J. Quantum Electron.* **30**(4), 1122–1131 (1994).
14. N. K. Das, Y. Yamayoshi, and H. Kawaguchi, "Analysis of basic four-wave mixing characteristics in semiconductor optical amplifier by the finite-difference beam," *IEEE J. Quantum Electron.* **36**(10), 1184–1192 (2000).

15. K. E. Zoiros, C. Riordan, and M. J. Connelly, "Semiconductor optical amplifier pattern effect suppression using a birefringent fiber loop," *IEEE Photon. Technol. Lett.* **22**(4), 221–223 (2010).
16. J. A. Constable et al., "Laser linewidth measurement using a Mach-Zehnder interferometer and an optical amplifier," *Electron. Lett.* **30**(2), 140–142 (1994).
17. K. Inoue, "Technique to compensate waveform distortion in a gain-saturated semiconductor optical amplifier using a semiconductor saturable absorber," *Electron. Lett.* **34**(4), 376–378 (1998).
18. T. Durhuus, B. Mikkelsen, and K. E. Stubkjaer, "All-optical wavelength conversion by semiconductor optical amplifiers," *IEEE J. Lightwave Technol.* **14**(6), 942–954 (1996).
19. R. J. Manning and D. A. O. Davies, "Three-wavelength device for all-optical signal processing," *Opt. Lett.* **19**(12), 889 (1994).
20. S. Banerjee et al., "A polarization multiplexing technique to mitigate WDM crosstalk in SOAs," *IEEE Photon. Technol. Lett.* **12**(10), 1415–1416 (2000).
21. L. F. Tiemeijer et al., "Reduced intermodulation distortion in 1300 nm gain-clamped MQW laser amplifiers," *IEEE Photon. Technol. Letts.* **7**(3), 284 (1995).
22. D. Wolfson et al., "Detailed theoretical investigation of the input power dynamic range for gain-clamped semiconductor optical amplifier gates at 10 Gb/s," *IEEE Photon. Technol. Lett.* **10**(9), 1241–1243 (1998).
23. Q. Xu et al., "Interferometric method of suppressing the pattern effect in a semiconductor optical amplifier," *Opt. Lett.* **25**(21), 1597–1599 (2000).
24. K. E. Zoiros, T. Siarkos, and C. S. Koukourlis, "Theoretical analysis of pattern effect suppression in semiconductor optical amplifier utilizing optical delay interferometer," *Opt. Commun.* **281**(14), 3648–3657 (2008).
25. J. Yu and P. Jeppesen, "Improvement of cascaded semiconductor optical amplifier gates by using holding light injection," *IEEE J. Lightwave Technol.* **19**(5), 614–623 (2001).
26. Q. Xu et al., "Experimental demonstration of pattern effect compensation using an asymmetrical Mach-Zehnder interferometer with SOAs," *Photon. Technol. Lett.* **13**(12), 1325–1327 (2001).
27. R. M. Silva et al., "Theoretical and experimental results of high-birefringent fiber loop mirror with an output port probe," *IEEE J. Lightwave Technol.* **30**(8), 1032–1036 (2012).
28. J. Xu, X. Zhang, and J. Mørk, "Investigation of patterning effects in ultrafast SOA-based optical switches," *IEEE J. Quantum Electron.* **46**(1), 87–94 (2010).
29. M. Y. Hong et al., "Femtosecond self- and cross-phase modulation in semiconductor laser amplifiers," *IEEE J. Sel. Topics Quantum Electron.* **2**(3), 523–539 (1996).
30. N. K. Das, H. Kawaguchi, and M. Razaghi, "Optical phase-conjugation of picosecond four-wave mixing signals in SOAs," Chapter 5 in *Optical Communication*, N. Das, Ed., pp. 86–112, InTech, Austria (2012).
31. M. Razaghi, V. Ahmadi, and M. J. Connelly, "Comprehensive finite-difference time-dependent beam propagation model of counter-propagation picosecond pulses in a semiconductor optical amplifier," *IEEE J. Lightwave Technol.* **27**(15), 3162–3174 (2009).
32. R. S. Tucker, G. Eisenstein, and S. K. Korotky, "Optical time-division multiplexing for very high bit-rate transmission," *IEEE J. Lightwave Technol.* **6**(11), 1737–1749 (1988).
33. R. Yin, J. Teng, and S. Chua, "A 1×2 optical switch using one multimode interference region," *Opt. Commun.* **281**(18), 4616–4618 (2008).

Mohammad Razaghi received his PhD in electronics engineering from Tarbiat Modares University, Tehran, Iran, in 2009. Currently, he is working as an assistant professor at the Department of Electrical and Computer Engineering, University of Kurdistan, Sanandaj, Iran. His current research interests include quantum photonics devices. He is the author or coauthor of several articles in international technical journals and conferences. He is a regular reviewer of several international technical journals and conference papers.

Omid Jafari received his BSc degree in electronics engineering from University of Kurdistan, Sanandaj, Iran, in 2012. Currently, he is working toward his MSc degree in microwave communication in Sharif University of Technology, Tehran, Iran. His research interests include nonlinear optic, high-speed communication devices, analysis and design of photonic devices, synthesis and design of microwave filter and multiplexers, and microwave tubes.

Narottam K. Das received his PhD in electrical engineering from Yamagata University, Japan in 2000. Currently, he is an associate professor at the Department of Electrical and Computer Engineering, Curtin University, Sarawak Malaysia. Earlier, he worked at Curtin University, Edith Cowan University, Monash University, Australia; NEC Japan; and BEXIMCO, Bangladesh. His research interests include pulse propagation, wave-mixing, high-speed communication devices and plasmonics. He is the editor of the books Optical Communication Systems and Optical Communication.